Journal of Functional Foods 66 (2020) 103776

Contents lists available at ScienceDirect

Journal of Functional Foods

journal homepage: www.elsevier.com/locate/jff

Preparation of corn glycopeptides and evaluation of their antagonistic effects on alcohol-induced liver injury in rats

Xiao-jie Wang[a,b], Xiao-lan Liu[a,b,*], Xi-qun Zheng[c], Yue Qu[b], Yan-guo Shi[a,*]

[a] Key Laboratory of Food Science and Engineering of Heilongjiang Province, Harbin University of Commerce, Harbin 150076, PR China
[b] Key Laboratory of Corn Deep Processing Theory and Technology of Heilongjiang Province, College of Food and Bioengineering, Qiqihar University, Qiqihar 161006, PR China
[c] Heilongjiang Bayi Agricultural University, Daqing 163319, PR China

ARTICLE INFO

Keywords:
Zein
Transglutaminase
Glycopeptide
Alcohol metabolism
Hepatoprotective effect

ABSTRACT

New glycosylated zein peptides (GZP) were produced by transglutaminase-induced D-glucosamine conjugation onto zein peptides. GZP's antagonistic effects on alcohol-induced liver injury in rats were evaluated. Compared with the alcohol model group, GZP (250 mg/kg·bw) remarkably increased alcohol dehydrogenase, acetaldehyde dehydrogenase, endogenous antioxidant enzymes activities, and GSH levels in liver, decreased serum triacylglycerol, tumor necrosis factor-α, liver malonaldehyde, reactive oxygen species, and lipopolysaccharide (LPS) levels, and significantly reversed pathological changes in liver tissues. These results indicate that low-dose GZP administration can alleviate alcohol-induced liver injury by accelerating alcohol metabolism, reversing hepatic redox status, and attenuating LPS-mediated inflammation responses. GZP is a potential alcohol metabolism promoter and liver-protective agent.

1. Introduction

Corn gluten meal (CGM) is a co-product of corn wet-milling process and contains approximately 67–71% proteins including zein, glutenin, globulin, and albumin. Alcohol-soluble zein accounts for 65–68% of CGM proteins (Gioia, Cuq, & Guilbert, 1998). Zein contains 8.3–10.52% Ala, 19.3–25% Leu, 9.0–10.53% Pro, 21.4–31.3% Glu, and 6.8–7.6% Phe (Pomes, 1971). These amino acids play extremely important roles in accelerating alcohol metabolism, exerting antioxidant effects, and affording hepatic protection (Jiang, Zhang, Lin, & Cheng, 2018, Yamaguchi, Takada, Nozaki, Ito, & Furukawa, 1996, Yang, Ito, Morimatsu, Furukawa, & Kimura, 1993). However, insolubility of zein in aqueous phase severely limits its application in food industry. Therefore, modification of zein is necessary to increase its solubility, release its functionalities, and expand its applications in functional food industry.

Microbial transglutaminase (TGase) is an acyltransferase, it catalyzes cross-linking between protein (or peptide) molecules and is widely used in dairy and meat processing sectors of food industry. In TGase-catalyzed acyl-transfer reaction, γ-carboxyamide group of Gln acts as acyl donor, ε-amino group of Lys as acyl acceptor (Kieliszek & Misiewicz, 2014). TGase also catalyzes glycosylation between protein and sugar containing primary amine such as D-glucosamine or chitosan, as acyl acceptor. Recently, TGase-mediated protein glycosylation has been applied for the modification of food proteins such as soy protein, casein, whey protein, and corn protein (Chen et al., 2017, Jiang & Zhao, 2010; Shi & Zhao, 2019, Wang et al., 2017). The glycosylation between zein and D-glucosamine has been preliminary investigated by our laboratory, however, only 11.34 mg of D-glucosamine was covalently conjugated onto 1 g of zein (Zhou, Liu, Liu, & Zheng, 2014), the poor solubility of zein in aqueous solution limited its conjugating capacity to D-glucosamine.

Abbreviations: ADH, alcohol dehydrogenase; ALDH, acetaldehyde dehydrogenase; ALT, alanine aminotransferase; AST, aspartate aminotransferase; ZP, zein peptide; GZP, glycosylated zein peptide; CP, corn peptide; CGM, corn gluten meal; DNS, 3,5-dinitrosalicylic acid; FID, flame ionization detector; FTIR, Fourier-transform infrared; GSH, glutathione; GSH-Px, glutathione peroxidase; GSR, glutathione reductase; GSSG, glutathione disulfide; IL, interleukin; INF, interferon; KBr, potassium bromide; LPS, lipopolysaccharide; MDA, malonaldehyde; NAD, nicotinamide adenine dinucleotide; NF-κB, nuclear factor-kappa B; ROI, reactive oxygen intermediate; ROS, reactive oxygen species; SOD, superoxide dismutase; SPI, soybean protein isolate; TG, triacylglycerol; TGase, transglutaminase; TNF, tumor necrosis factor; Nrf2, nuclear factor-erythroid 2-related factor 2

* Corresponding authors at: College of Food Engineering, 138 Tongda Street, Daoli District, Harbin, Heilongjiang Province 150076, PR China (Yan-guo Shi). College of Food and Bioengineering, 42 Wenhua Street, Qiqihar, Heilongjiang Province 161006, PR China (Xiao-lan Liu).
E-mail addresses: liuxiaolan001@126.com (X.-l. Liu), yanguosh@163.com (Y.-g. Shi).

https://doi.org/10.1016/j.jff.2019.103776
Received 2 August 2019; Received in revised form 27 December 2019; Accepted 30 December 2019
Available online 24 January 2020

Hydrolysis of CGM catalyzed by proteases increased its solubility remarkably (Zhu, He, & Hou, 2019). The hydrolysates (corn peptides, CP) from CGM possess multiple bioactive functions including facilitating alcohol metabolism, increasing antioxidant levels, and inhibiting angiotensin I-converting enzyme activity (Yamaguchi et al., 1996, Jiang et al., 2018, Zhou et al., 2013). Additionally, CP administration before alcohol intake decreased blood alcohol levels significantly in both stroke-prone spontaneously hypertensive rats (dose: 1 g/kg·bw) and humans (dose: 5 g/day) (Yamaguchi et al., 1996, Yamaguchi, Nishikiori, Ito, & Furukawa, 1997). Moreover, in a murine model, CP (range from 200 mg/kg·bw to 1 g/kg·bw) shown a significant protection against liver injuries induced by alcohol, Bacillus Calmette-Guerin/lipopolysaccharide (LPS), and carbon tetrachloride (Guo, Sun, He, Yu, & Du, 2009, Lv et al., 2013, Yu, Li, He, Huang, & Zhang, 2013). Those results provide referential data for CP's application in functional foods. But above mentioned effective doses are still somewhat too much, it is necessary to search new technical approaches to reduce effective functional doses of modified products from CGM.

In the present study an approach of combining hydrolysis and glycosylation was conducted to increase zein solubility and efficiency as functional food. Zein was hydrolyzed by Alcalase to form zein peptide (ZP), and then ZP was glycosylated by microbial TGase, D-glucosamine as the acyl acceptor, to prepare new glycosylated zein peptides (GZP). GZP's activities of promoting alcohol metabolism *in vitro* and *in vivo* as well as the antagonistic effects on alcohol-induced chronic liver injury in Wister rats were evaluated.

2. Materials and methods

2.1. Materials and chemicals

Zein and 2-deoxy-D-ribose were obtained from Sigma-Aldrich (St. Louis, MO, USA). Microbial TGase (1000 U/g) was purchased from Jiangsu Yiming Biological Co. (Jiangsu, China). Pepsin, trypsin, and D-glucosamine hydrochloride were purchased from Sangon Biotech (Shanghai, China). Alcalase (6.28×10^5 U/mL) was a gift from Novo Nordisk (Bagsvaerd, Denmark). Alcohol dehydrogenase (ADH) and nicotinamide adenine dinucleotide (NAD^+) were purchased from Baoman Biotech (Shanghai, China), and absolute alcohol and *tert*-butanol (chromatographic purity) were purchased from Sinopharm Group (Shanghai, China). All other chemicals and reagents used were of analytical grade.

2.2. ZP preparation

Briefly, 40 g of zein was suspended in 800 mL of distilled water and placed in a 60 °C water bath with magnetic stirring. The pH of the suspension was adjusted to 8.5, and 1.20 g of Alcalase was added to initiate enzymatic hydrolysis, during which the pH of the reaction was maintained at 8.5 by the continuous addition of 1 M NaOH. After 2 h, the reaction was terminated by heating in a boiling water bath for 10 min. The hydrolysate was centrifuged at 4000*g* for 10 min, and ZP was obtained by freeze-drying the supernatant. The degree of hydrolysis of zein was 23.99 ± 0.21%, as determined using the pH-stat method. ZP contained 81.86 ± 0.50% protein with a molecular-weight distribution of 300 to 6390 Da, 0.59 ± 0.01% carbohydrate, 0.73 ± 0.01% fat, 11.17 ± 0.10% ash, and 5.65 ± 0.27% water.

2.3. ZP glycosylation

ZP glycosylation was performed in a water bath with constant agitation. Briefly, ZP was made into a solution with a certain substrate concentration, which was followed by the addition of D-glucosamine, mixing, heating to the appropriate temperature, and adjustment to the appropriate pH. TGase was then added to initiate the enzymatic glycosylation reaction. The following parameters were varied in the glycosylation reaction: pH was varied at 0.3 intervals from 7.4 to 8.3; temperature was varied at 4 °C intervals from 36 to 48 °C; ZP concentration was varied at 1% intervals from 1% to 4%; D-glucosamine dosage was varied according to the mass ratio of ZP to D-glucosamine (1:0.5, 1:1, 1:2, 1:3, and 1:4); the enzyme:substrate ratio was varied at 10 U/g intervals from 30 to 70 U/g; reaction time was varied at 1 h intervals from 5 to 9 h. Following glycosylation, the reaction mixture was immediately heated at 85 °C for 5 min to deactivate TGase. The reaction mixture was then dialyzed for 48 h at 4 °C using a Float-A-Lyzer G2 dialysis device with a molecular weight cut off of 100–500 Da (CE, 10 mL, Sangon Biotech, Shanghai, China) against distilled water to remove excess D-glucosamine. GZP was obtained by freeze-drying the dialysate and was stored in a desiccator for further analysis.

2.4. Measurement of the degree of D-glucosamine conjugation in GZP

A 3,5-dinitrosalicylic acid (DNS) assay was used to determine the amount of D-glucosamine conjugated onto ZP. A GZP sample (0.01 g) was placed in an ampoule, after which 2.5 mL of 6 M HCl was added. The sample was then acid-hydrolyzed at 100 °C for 7.5 h in a nitrogen environment, and the hydrolysate was filtered through Whatman No. 1 filter paper (Whatman International, Ltd., Maidstone, UK) into a centrifuge tube. Then 0.7 mL of 6 M NaOH and 1.5 mL of DNS reagent were added to 0.8 mL of the filtrate, and the mixture was maintained in a boiling water bath for 5 min. The tubes were immediately cooled to room temperature (22 ± 2 °C). Next, 1 mL of distilled water was added to the solution and mixed thoroughly by shaking, followed by the measurement of absorption at 540 nm. A blank solution without a test sample was also prepared as a control. A D-glucosamine calibration curve was generated and used to calculate the D-glucosamine content of GZP and the results were expressed as units of mg D-glucosamine per g of ZP.

2.5. Fourier-transform infrared (FTIR) and intrinsic fluorescence spectroscopies of GZP

GZP and ZP were characterized by FTIR and intrinsic fluorescence spectroscopies to confirm enzymatic glycosylation.

The sample was mixed with potassium bromide (KBr) to prepare pressed KBr disks; the IR absorptions of these disks were measured using an FTIR spectrometer (Spectrum One FTIR; PerkinElmer, Norwalk, CT, USA). The scan range, resolution, and wavenumber precision were 400 to 4000 cm^{-1}, 4 cm^{-1}, and 0.01 cm^{-1}, respectively, and 32 scans were performed at an environmental temperature of 25 °C, with KBr used as a blank.

The intrinsic fluorescence spectra of GZP and ZP were recorded with a ZSX fluorescence spectrophotometer (Rigaku, Japan) at wavelengths of 336 nm (excitation) and 362–500 nm (emission), using 15 nm as a constant slit. Samples were dissolved in deionized water at a concentration of 0.1 mg/mL (protein basis). The intrinsic fluorescence of samples was assessed in a rectangular quartz cuvette with a 1 cm pathlength at room temperature (22 ± 2 °C). Deionized water was used as the blank for all samples.

2.6. Determination of the amino acid composition of GZP

The amino acid compositions of GZP and ZP were determined using an L-8900 automatic amino acid analyzer (Hitachi, Tokyo, Japan). A sample (0.5 g) was mixed with 6 M HCl and digested for 22 h at 110 °C in a nitrogen atmosphere, and then cation-exchange chromatography and ninhydrin derivatization were performed on the hydrolysate. The amino acid composition of the sample was expressed in units of g per 100 g of protein.

2.7. In vitro activity of GZP in promoting alcohol metabolism

The hydroxyl-radical-scavenging proportion and the ADH activation rate were used to characterize the *in vitro* activity of GZP in promoting alcohol metabolism. Additionally, the effect of *in vitro*-simulated gastrointestinal digestion on the promotion of alcohol metabolism was investigated.

The hydroxyl-radical-scavenging proportion was measured using a previously reported method (Wang et al., 2014). The ADH activation rate was measured using the enzymatic assay method described by Vallee and Hoch (1955), with minor modifications. Briefly, 1.5 mL of 32 mmol $Na_4P_2O_7$ buffer (pH 8.8), 1.0 mL of 27 mM NAD^+, 0.5 mL of 11.5% alcohol (v/v), and 0.1 mL of the sample solution were added to a test tube. After thorough mixing, the covered test tube was placed in a 25 °C water bath for 5 min, followed by addition of 0.1 mL of ADH (0.25 U/mL). The mixture was shaken thoroughly, scanned at 340 nm, and allowed to react for 5 min. The initial linear portion of the reaction was plotted, and its slope was recorded as Kp. For the control group, 0.1 mL of distilled water was used in place of the sample, with the slope recorded as Kc. For the blank, 0.5 mL of distilled water was used to replace 11.5% alcohol. The ADH activation rate was calculated using Eq. (1):

$$\text{ADH activation rate } (\%) = \left(\frac{K_p - K_c}{K_c}\right) \times 100\% \quad (1)$$

In vitro-simulated gastrointestinal digestion of GZP was determined according to the method reported by Song and Zhao (2013), with minor modifications. First, the pH of GZP solution with a substrate concentration of 3% (w/v) was adjusted to 2.0 using 12 M HCl. Pepsin was then added [2% (w/w), protein basis] to hydrolyze the substrate for 1.5 h at 37 °C. The pH of the solution was adjusted to pH 7.5 using 6 M NaOH, trypsin [4% (w/w), protein basis] was then added, and the solution was hydrolyzed at 37 °C for 4 h. The enzymes were inactivated immediately in a boiling water bath for 10 min and the hydrolysate was centrifuged at 4000*g* for 10 min. The supernatant was freeze-dried to obtain the digestion product, after which the hydroxyl-radical-scavenging proportion and the ADH activation rate were determined.

2.8. Measurement of GZP-mediated liver-protective effects in vivo

2.8.1. Animals

Eighty female Wistar rats (8-weeks-old; weight: 180–220 g) were purchased from the Changchun Yisi Experimental Animal Research Center (Changchun, China). The rats were reared in a standard environment at temperatures ranging from 19 to 26 °C, a relative humidity from 40% to 70%, alternating 12 h light/dark periods, and *ad libitum* access to food and water. Animal handling was performed in accordance with the *Guide for the Care and Use of Laboratory Animals* published by the U.S. National Institutes of Health (NIH Publication No. 85-23, 1996 revision).

After acclimation for 1 week, rats were randomly allocated into eight groups ($n = 10$/group) as follows: normal control, alcohol model, three GZP-supplemented groups (125 mg/kg·bw, 250 mg/kg·bw, and 500 mg/kg·bw), and three ZP-supplemented groups serving as positive controls (125 mg/kg·bw, 250 mg/kg·bw, and 500 mg/kg·bw). The normal control and model groups were fed a standard pellet diet (Changchun Yisi Experimental Animal Research Center, Changchun, China), whereas the GZP and ZP groups were fed a self-made pellet diet with low-, medium-, and high-dose GZP and ZP, respectively, in which excess mineral salts were removed by nanofiltration.

For self-made pellet diet preparation, the standard pellet diets were ground using a feed processor. The ground diet was divided into six groups and then GZP and ZP, at 125, 250 and 500 mg/kg·bw, were mixed with the ground feed, and the pellets were made with a small feed pelletizer (KL150, Zhengzhou, China).

The model group and the six intervention groups were subjected to intragastric administration of 50° Baijiu (Chinese liquor; Heilongjiang Beidacang Group Co., Ltd, Qiqihar, China) once daily for 28 consecutive days. The dose of the intragastrically administered alcohol was gradually increased throughout a 4-week feeding period, with a dose of 8 mL/kg·bw in the first week, 10 mL/kg·bw in the second week, 12 mL/kg·bw in the third week, and 15 mL/kg·bw in the fourth week. The normal control group was intragastrically administered corresponding quantities of 0.9% normal saline. Body weight was measured once per day during the experimental period.

2.8.2. Measurement of blood alcohol concentrations in rats

On day 21 of the experiment, 1 mL of blood was collected from each rat via the tail vein 15 min after the rats were subjected to the intragastric administration of alcohol, and the blood sample was placed in a medical anticoagulation tube. Tert-butanol (internal standard) solution (100 μL; 4 mg/mL) was added to the sample, which was shaken until uniformly mixed. The mixture (2 μL) was then rapidly aspirated and injected into a gas chromatography (GC122, Shanghai Precision & Scientific Instrument Co., Ltd, Shanghai, China) equipped with a flame ionization detector (FID) (Shanghai Precision & Scientific Instrument Co., Ltd, China). The peak areas of alcohol and the internal standard were then determined using a gas chromatography column (GDX103; 2 m × 3 mm, 60–80 mesh; Chongqing Zhongpu Technology Co., Ltd, Chongqing, China) at a column temperature of 180 °C. The conditions of the FID system were as follows: hydrogen gas, 30 mL/min; air, 3000 mL/min; auxiliary: nitrogen gas, 40 mL/min; and temperature, 200 °C. The blood alcohol level of each rat was determined using the ratio of the peak area of alcohol to the peak area of the internal standard, and the standard curve was plotted using various alcohol concentrations. The results were expressed in units of μg/g.

2.8.3. Determination of biochemical parameters

The intragastric administration of alcohol to the rats was continued until day 28, at which time the rats were fasted for 12 h before sacrificing via cervical dislocation. Blood samples were collected and serum was isolated for further analysis. After the livers were weighed, and then were dissected into two portions, one portion was used for histopathologic analysis and the other portion was homogenized in ice-precooled 0.9% normal saline to form a 10% liver homogenate.

Aspartate aminotransferase (AST) and alanine aminotransferase (ALT) activities as well as triacylglycerol (TG) levels in the serum were measured using an automated biochemical analyzer (Hitachi 7020; Hitachi, Tokyo, Japan). Enzyme-linked immunosorbent assay kits (Jianglaibio, Shanghai, China) were used according to the manufacturer's instructions to measure tumor necrosis factor (TNF)-α, interleukin (IL)-6, and interferon (IFN)-γ levels in the serum, as well as ADH, aldehyde dehydrogenase (ALDH), superoxide dismutase (SOD), glutathione (GSH)-disulfide (GSSG) reductase (GSR), and GSH peroxidase (GSH-Px) activities as well as reactive oxygen species (ROS), malondialdehyde (MDA), LPS, and GSH levels in the liver homogenates.

2.8.4. Histopathologic analysis

Fresh liver tissues were fixed in 10% formaldehyde, dehydrated, and embedded in paraffin. The embedded tissues were then sliced into 4 μm sections, which were stained with standard hematoxylin and eosin, and visualized using an Olympus BX43 microscope (Olympus, Tokyo, Japan).

2.9. Statistical analysis

All quantitative data were expressed as the mean ± standard deviation (SD), and statistical comparisons were performed using one-way analysis of variance and Tukey's test. Differences were considered statistically significant at $P < 0.05$.

3. Results and discussion

3.1. GZP preparation

D-glucosamine, a compound produced from the substitution of a hydroxyl group in glucose with an amino group, is currently extracted primarily from crustaceans such as prawns and crabs (Hrynets, Ndagijimana, & Betti, 2014). The free amine group of D-glucosamine enables its incorporation into food proteins/peptides to form glycosylated proteins/glycopeptides via TGase. In this study, ZP was modified using TGase in the presence of D-glucosamine to prepare GZP. To maximize the conjugation degree of D-glucosamine onto ZP, various conditions for the glycosylation reaction were investigated and a DNS assay was used to determine the degree of conjugation onto ZP. Suitable glycosylation conditions were determined as follows: initial pH, 7.7; temperature, 44 °C; substrate concentration, 3%; ZP/D-glucosamine mass ratio, 1:3; TGase, 50 U/g of protein; reaction time, 7 h. Under the optimal conditions, the amount of D-glucosamine conjugated to ZP was 149.22 mg/1 g of ZP. Previous studies have investigated TGase-mediated glycosylation between plant proteins and D-glucosamine. Jiang and Zhao (2010) reported the conjugation of 3.3 mol of D-glucosamine onto 1 mol of soybean protein isolate (SPI) (equivalent to 2.62 mg/g SPI) by TGase, and Yao and Zhao (2016) reported a glycosylated SPI containing D-glucosamine at 19.7 mg/g protein. In the present study, we observed a higher degree of D-glucosamine conjugation onto ZP compared to earlier reports, suggesting relatively little steric hindrance by peptides compared with proteins against D-glucosamine conjugation, and greater exposure of additional reactive sites normally embedded within proteins.

3.2. FTIR and intrinsic fluorescence analysis of GZP

FTIR and intrinsic fluorescence spectroscopies were performed to confirm enzymatic glycosylation between D-glucosamine and ZP.

The FTIR spectra of GZP and ZP, shown in Fig. 1, indicated that in the range of 1080–1206 cm^{-1}, GZP differed from ZP, especially at 1085 cm^{-1}, where the stretching vibration of GZP was significantly stronger. Recent FTIR analysis of compounds suggested that peaks approaching a range of 1000–1200 cm^{-1} are attributed to two types of C–O stretching vibrations, i.e. ring C–O–H and pyranose C–O–C (Paluszkiewicz, Stodolak, Hasik, & Blazewicz, 2011). In the present study, the presence of the characteristic pyranose absorption peak in the GZP spectrum and its absence in the ZP spectrum indicated covalent conjugation of some D-glucosamine onto ZP during TGase-catalyzed glycosylation.

The fluorescence emission spectra of GZP and ZP are shown in Fig. 2. Following excitation at 336 nm, ZP exhibited a fluorescence

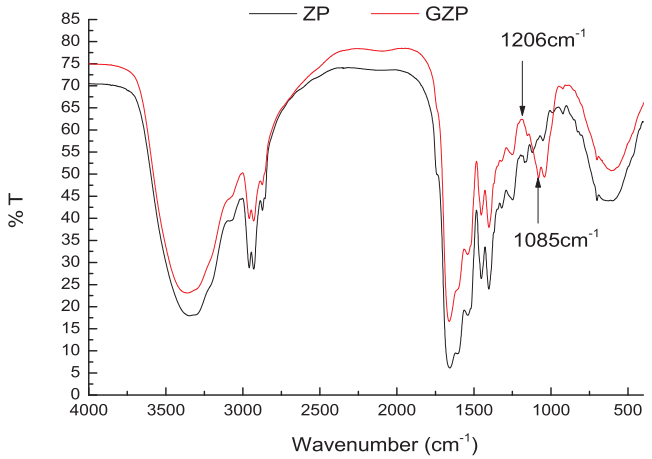

Fig. 1. FT-IR spectra of GZP and ZP.

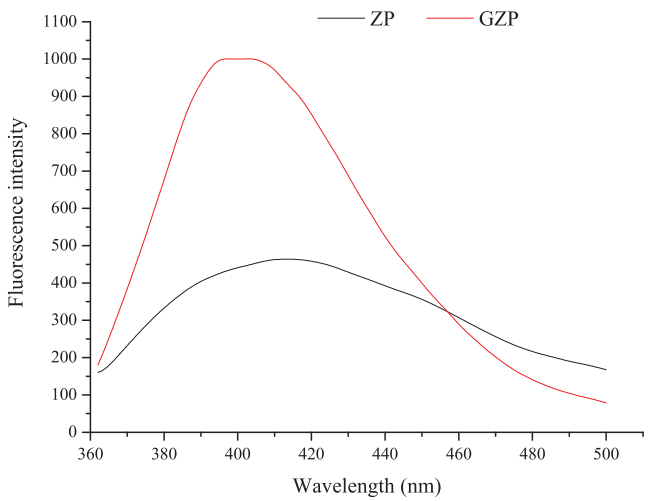

Fig. 2. The fluorescence emission spectra of GZP and ZP.

emission maximum at 413 nm. The intrinsic fluorescence intensity of the glycosylated sample reached a maximum that was approximately 54% higher than that of ZP. Hong, Gottardi, Ndagijimana, and Betti (2016) also found that in the presence of TGase, glycated poultry meat protein hydrolysates with D-glucosamine had higher fluorescence intensity than that of the native hydrolysate. The increase of fluorescence intensity might be induced by D-glucosamine conjugation on ZP, which led to relatively large molecular weight ZP unfolding and the exposure of more nonpolar amino acids such as Trp, Tyr and Phe to the molecular surface. When Chen and Wang (2019) investigated the cryoprotective activities of antifreeze glycopeptide analogues (GAPP) obtained by nonenzymatic glycation, found that the relative fluorescence intensity of GAPP enhanced, compared with antifreeze peptide (APP), they speculated that APP covalently linkage to dextran caused part of the chromophore exposure to the molecular surface, resulting in fluorescence intensity increase.

Moreover, the glycosylation reaction led to a blue-shifted wavelength of the maximum emission (from 413 to 400 nm), indicating that the polarity of the aromatic amino acids microenvironment had changed after glycosylation. The phenomenon of intrinsic fluorescence blue shift was also observed when tropomyosin was modified with TGase and D-glucosamine (Yuan et al., 2017). Above results indicated that TGase-catalyzed glycosylation altered the special conformations of ZP, and provided indirect evidence of enzymatic glycosylation between D-glucosamine and ZP.

3.3. Amino acid composition of GZP

The amino acid compositions of GZP and ZP are shown in Table 1. GZP and ZP had similar amino acid compositions and were rich in Glu (18.34% and 16.11%, respectively), Leu (15.51% and 13.85%, respectively), Ala (7.36% and 6.46%, respectively), and Pro (6.56% and 5.55%, respectively). It should be pointed out that although GZP was dialyzed after the glycosylation by a 100–500 Da cut off molecular weight membrane in order to remove unreacted D-glucosamine, but the dialysis exhibited a small influence on GZP' amino acid composition just because the ingredient < 300 Da in ZP was 4.1% (data not shown). It must be emphasized that the amino acid compositions of GZP and ZP are unique. Previous studies found that the ingestion of individual Ala, Leu, and Pro reduced blood alcohol levels in stroke-prone spontaneously hypertensive rats and humans (Yamaguchi, Takada, Nozaki, Ito, & Furukawa, 1996), and both Ala and Gln relieved health impairment caused by constant or massive alcohol intake (Kawada, Masaki, Mori, & Torii, 1988). These findings indicate that GZP might play important roles in accelerating alcohol metabolism.

Table1
Amino acid composition of GZP and ZP.

Amino acid	ZP (g/100 g protein)	GZP (g/100 g protein)
Asp	3.59	3.93
Thr	1.82	2.03
Ser	3.22	3.34
Glu	16.11	18.34
Gly	0.97	0.98
Ala	6.46	7.36
Cys	0.15	0.21
Val	2.66	3.16
Met	1.21	1.89
Ile	2.86	3.24
Leu	13.85	15.51
Tyr	3.45	3.84
Phe	4.68	5.33
Lys	0.13	0.25
His	1.02	1.23
Arg	0.98	1.10
Pro	5.55	6.56
Total	68.68	78.31

3.4. GZP-related promotion of alcohol metabolism in vitro

Most alcohol absorbed into the blood is metabolized in the liver via the ADH pathway, which involves both ADH and ALDH, with the blood alcohol elimination rate usually depending on the activity of hepatic ADH. Fig. 3a shows the effect of ZP glycosylation and *in vitro* digestion of GZP on the ADH activation rate. Both ZP glycosylation and *in vitro* digestion of GZP significantly increased the ADH activation rate. At 2 mg/mL GZP, the ADH activation rate was 14.54%, which was 9.3% higher than that of ZP. Additionally, the ADH activation rate of the digested GZP at the same concentration was 38.03%, which was 23.49% higher than that of pre-digested GZP. A possible explanation for the increased ADH activity is that GZP induced changes of the ADH structure might favor alcohol binding in the active site. Furthermore, compared with GZP, the digested GZP exhibited relatively low steric hindrance to ADH, which was important for stabilizing ADH activity. On the other hand, the antioxidant activity of the digested GZP was remarkably increased, it might protect ADH from oxidative inactivation.

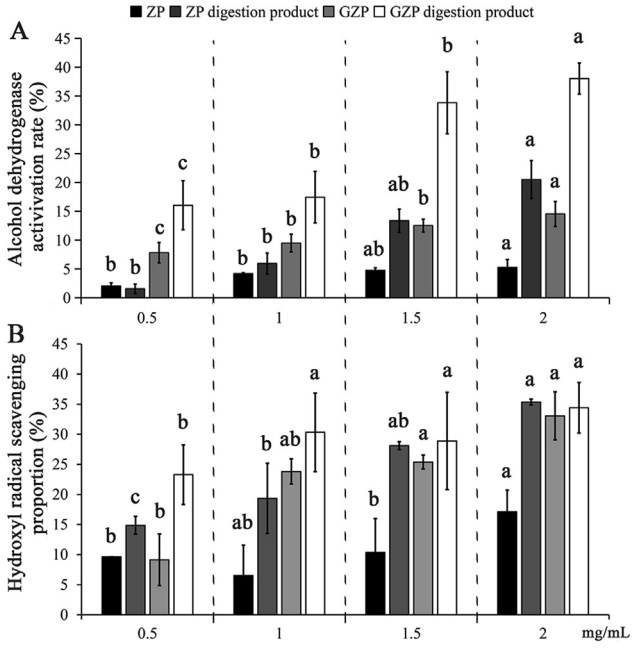

Fig. 3. *In vitro* activity of GZP and ZP in promoting alcohol metabolism. (A) ADH activation rate; (B) hydroxyl radicals scavenging proportion. Data are expressed as the mean ± SD, and differences were analyzed by Tukey's test, n = 3. The results without common superscript letters were statistically different ($P < 0.05$).

Alcohol metabolism produces large amounts of free radicals such as hydroxyl radicals, which promote oxidative stress in liver cells. Fig. 3b shows the effect of ZP glycosylation on its hydroxyl-radical-scavenging ability. The results showed that glycosylation significantly improved ZP-specific scavenging ability, which might be attributed to the following activities: (1) the D-glucosamine moiety of GZP discontinued free radical chain reactions by donating additional protons and/or (2) GZP acted as a chelating agent for Fe^{2+} to disrupt either the Fenton reaction or the Haber-Weiss reaction, thereby suppressing the generation of hydroxyl radicals. Additionally, it was observed that *in vitro* digestion did not disrupt GZP-related hydroxyl-radical scavenging abilities, which might be attributed to the amino acid composition of GZP. Ren, Liang, et al. (2018) found that CP containing Pro, Glu, and Asp were strongly resistant to digestion. These results indicated that GZP has an edge in attenuating liver damage caused by increases in alcohol-induced hydroxyl radicals.

3.5. GZP-mediated protection against alcohol-induced liver injury in rats

3.5.1. GZP-specific promotion of alcohol metabolism in vivo

The effects of GZP on hepatic ADH and ALDH activities are shown in Fig. 4. Compared with the normal control group, the ADH and ALDH activities of the model group decreased by 37.11% and 34.11%, respectively, resulting in lower rates of oxidative metabolism of alcohol and increased alcohol-related toxic effects on the liver. Compared with the model group, GZP at 250 mg/kg·bw increased ADH and ALDH activities by 55.97% and 25.51%, respectively, whereas ZP at the same dose increased ADH and ALDH activities by 39.87% and 24.16%, respectively, indicating that GZP and ZP were both capable of accelerating alcohol and acetaldehyde metabolism in the liver to reduce hepatotoxicity, while GZP exhibited more remarkable effect of accelerating alcohol metabolism. Ma, Hou, Shi, Liu, and He (2015) previously studied the effects of CP (prepared by Alcalase hydrolysis for 5 h) on alcohol-induced hepatocyte apoptosis in Kunming mice, and found significant downregulation of ADH and ALDH levels in the model group relative to the corresponding normal group, whereas these levels in the test group (CP at 200 mg/kg·bw) were significantly upregulated.

GZP's characteristics of accelerating alcohol and acetaldehyde metabolism might be attributed to its particular functional groups and amino acid composition. Previous studies reported that hydrophobic short-chain amide compounds (e.g. butyramide and valeramide) can enhance the alcohol-oxidizing activity of purified mouse class III ADH (Haseba et al., 2006). GZP (average hydrophobicity value: 6.12 kJ/mol, data not shown) harbors numerous amide linkages. The linkages are contributed by hydrophobic short-chain peptides, covalent conjugation between ZP and D-glucosamine, and cross-linkage between ZP. Therefore, the observed GZP-mediated increase of ADH and ALDH activities might be due to the presence of similar functional groups. On the other hand, the regulatory effect of GZP and ZP on ADH activities would be associated with GZP' and ZP' special amino acid composition. The oxidation of alcohol catalyzed by ADH requires the coenzyme NAD^+, which is an electron acceptor. GZP and ZP are rich in Glu, Leu, Ala, and Pro (Table 1). The oxidative metabolism of Glu and Pro carbon skeletons results in an increase in α-ketoglutarate; meanwhile, the oxidative metabolism of Leu and Ala carbon skeletons leads to an increase in acetyl coenzyme A. As a result, the tricarboxylic acid (TCA) cycle is strengthened, mitochondrial respiratory chain reactions are intensified, the regeneration of NAD^+ from NADH speeds up, and therefore ADH activities would be upregulated.

The GZP-related promotion of alcohol metabolism was confirmed by measuring blood alcohol levels in rats. After 15 min of intragastric administration of alcohol, the blood alcohol level in rats of the model

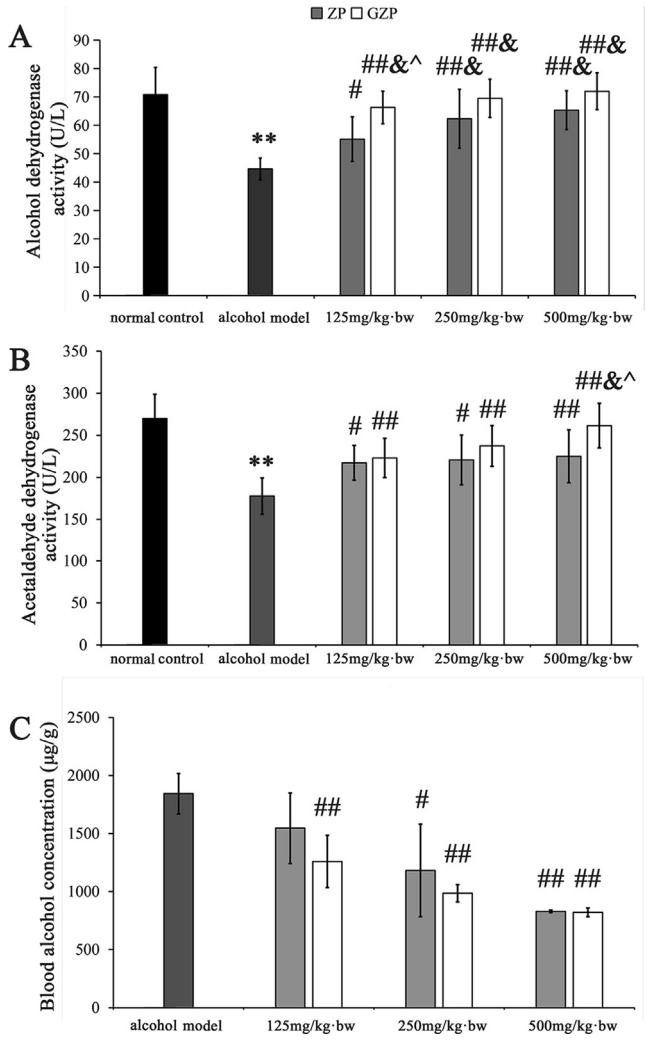

Fig. 4. *In vivo* activity of GZP and ZP in promoting alcohol metabolism. (A) liver activities of ADH; (B) liver activities of ALDH; (C) blood alcohol concentrations of rats. Data are expressed as the mean ± SD, and differences were analyzed by Tukey's test, n = 10. * $P < 0.05$ and ** $P < 0.01$ vs the normal control group, # $P < 0.05$ and ## $P < 0.01$ vs the alcohol model group, & $P > 0.05$ vs the normal control group, ^ $P < 0.05$ vs the same concentration of ZP.

group was 1844.07 μg/g, whereas that in rats administered low (125 mg/kg·bw), medium (250 mg/kg·bw), and high (500 mg/kg·bw) doses of GZP was 1259.46 μg/g, 985.66 μg/g, and 820.84 μg/g, respectively (Fig. 4c). At a dose of 250 mg/kg·bw, GZP intervention reduced blood alcohol levels by 46.55%, whereas ZP at the same dose reduced levels by 35.92% relative to those in the model group. Additionally, GZP intervention accelerated alcohol metabolism in the liver by upregulating hepatic ADH, leading to a rapid decline in blood alcohol levels in a dose-dependent manner, and these effects were found to be superior to those of ZP. To the best of our knowledge, this represents the first report of the ability of TGase-catalyzed glycopeptides to accelerate alcohol metabolism in rats. Yu et al. (2013) investigated the effect of CP on blood alcohol concentrations in mice, and showed that a dose of 200 mg/kg·bw CP (< 5,000 Da) reduced blood alcohol concentrations by 45.1% compared to those in the model group. In the present study, our results indicate GZP-mediated acceleration of alcohol metabolism as a mechanism underlying its protective effects against alcohol-induced liver injury.

3.5.2. GZP alleviates alcohol-induced hepatotoxicity and blood lipid abnormalities

Body weight gains during the experiment are shown in Table 2. Rats grew steadily in all groups during the experimental period. Despite weight gain levels that were slightly reduced in the alcohol-treated group, as compared to those in the other groups, there was no significant difference among the eight groups ($P > 0.05$). Kumar, Dwivedi, Lahkar, and Jangra (2019) also observed that alcohol administration alone increased the body weights of rats.

The liver index (i.e. liver-to-body weight ratio) can reflect the degree of liver damage. Alcohol administration significantly increased the liver index compared with the normal group ($P < 0.01$), providing direct evidence of toxic injury to the rat liver. Compared with the model group, the administration of GZP at all tested doses significantly abolished alcohol-induced elevations in liver indices (Table 2), which illustrated that it could attenuate alcohol-induced liver injury.

ALT and AST are cytoplasmic enzymes, with ALT found mainly in liver cells and AST mainly in cardiac muscle. The altered permeability of the liver-cell membrane allows ALT and AST to enter circulation; therefore, serum ALT and AST activities represent conventional and sensitive indicators of liver damage. Compared with the normal control group, serum ALT and AST activities in the model group were elevated by 50.10% and 51.29%, respectively, implying that alcohol intake caused severe damage to liver-cell membranes and mitochondria (i.e. the intragastric administration of alcohol once daily for four consecutive weeks induced hepatotoxicity in rats). However, compared with the model group, serum ALT and AST activities in groups receiving 125 mg/kg·bw, 250 mg/kg·bw, or 500 mg/kg·bw GZP decreased by 38.21% and 23.24% , 41.83% and 30.92%, 47.40% and 41.16%, respectively, whereas activities in groups receiving 250 mg/kg·bw and 500 mg/kg·bw ZP decreased by 27.01% and 26.34%, 34.25% and

Table 2
Effects of GZP on body weight gain, liver index, activities of serum ALT and AST, liver MDA content and serum TG content.

Treatment groups	Body weight gain (g)	Liver index (mg/g)	ALT (U/L)	AST (U/L)	MDA (nmol/mL)	TG (mmol/L)
Normal control	25.90 ± 7.07	33.07 ± 3.30	69.16 ± 14.09	234.93 ± 51.77	1.88 ± 0.46	1.64 ± 0.28
Alcohol model	18.25 ± 12.79	40.38 ± 4.15**	103.81 ± 26.38**	355.43 ± 64.28**	3.84 ± 0.44**	3.01 ± 0.57**
ZP(125 mg/kg·bw)	19.78 ± 6.02	36.55 ± 3.53	117.37 ± 31.16	323.20 ± 72.25	3.55 ± 0.44	1.84 ± 0.36## &
ZP(250 mg/kg·bw)	27.50 ± 7.01	36.21 ± 4.74	75.77 ± 25.00# &	261.81 ± 71.68# &	3.09 ± 0.23#	1.71 ± 0.32## &
ZP(500 mg/kg·bw)	26.33 ± 7.42	35.69 ± 2.49# &	68.26 ± 12.23# &	220.05 ± 49.46# &	2.81 ± 0.64##	1.55 ± 0.31## &
GZP(125 mg/kg·bw)	21.88 ± 10.23	34.62 ± 3.35## &	64.14 ± 3.72## & ^	272.82 ± 23.22# &	3.03 ± 0.56#	1.79 ± 0.48## &
GZP(250 mg/kg·bw)	24.71 ± 7.48	34.83 ± 3.50## &	60.39 ± 15.59## &	245.52 ± 65.65## &	2.92 ± 0.52##	1.61 ± 0.29## &
GZP(500 mg/kg·bw)	24.57 ± 14.21	34.36 ± 2.76## &	54.6 ± 6.59## &	209.13 ± 27.12## &	2.65 ± 0.56##	1.49 ± 0.28## &

Data are expressed as the mean ± SD, n = 10.
*$P < 0.05$ and,
** $P < 0.01$ vs the normal control group,
# $P < 0.05$ and,
$P < 0.01$ vs the model group,
& $P > 0.05$ vs the normal control group,
^ $P < 0.05$ vs the same concentration of ZP.

38.09%, respectively, indicating that both GZP and ZP could suppress alcohol-induced elevations in serum ALT and AST activities (Table 2), and GZP was more effective than ZP. The significant decrease in serum marker enzymes following GZP and ZP intervention might be associated with their ability to scavenge highly active hydroxyl radicals derived from alcohol metabolism, thus neutralizing oxidative damage to hepatocytes and reducing inflammation.

MDA is a major reactive aldehyde generated by the ROS-induced peroxidation of polyunsaturated fatty acids in biological membranes. Hence, MDA content is reflective of the severity of hepatic injury following free radical attack (Guo et al., 2009). Table 2 shows that alcohol intake increased hepatocyte MDA content to 3.84 nmol/mL, which was 2.04-fold higher than that in the normal control group, indicating that alcohol intake increased oxidative stress in hepatocytes. GZP and ZP treatment attenuated increase in lipid-peroxidation levels, especially in the high-dose groups, in which MDA content decreased by 30.99% and 26.82%, respectively, relative to levels in the model group. A possible reason for these findings is that GZP and ZP possess strong free radical-scavenging activities and can inhibit free radical reactions, preventing excessive lipid peroxidation (Fig. 3). However, MDA levels in GZP and ZP intervention groups were still higher than those in the normal control group, which implies that GZP and ZP could, to a certain extent, reduce alcohol metabolism-induced elevations in MDA levels.

Serum TG content is a sensitive indicator of lipid metabolism, as hepatic steatosis or lipid-metabolism disorders in the liver lead to increase in TG content. As shown in Table 2, serum TG level in the model group was significantly elevated relative to that in the control group ($P < 0.01$), indicating that four consecutive weeks of intragastric alcohol administration leads to blood lipid-metabolism disorders in rats, which is the collective effect of alcohol-induced disorders on the TCA cycle, oxidative stress, and inflammatory responses. This result was also supported by pathological observations (Fig. 6B). However, the administration of GZP and ZP at each respective dose prevented increase in serum TG levels and or even restored levels to normal. The significant decrease in TG levels following GZP intervention might be explained as follows: (1) GZP might increase hepatocyte resistance to oxidative stress by scavenging intracellular ROS and activating the relevant signaling pathways required for cellular defense systems against oxidative stress, thereby preventing lipid-metabolic disorders caused by mitochondrial damage in liver cells, (2) GZP might provide a potential supply of NAD^+ via the metabolism of Glu, Leu, Ala, and Pro, thereby accelerating lipid β-oxidation through adjustments to the NADH:NAD^+ ratio, which would consequently reduce TG accumulation in liver cells, and/or (3) TNF-α is known to increase intra-hepatic fat deposition by upregulating sterol regulatory element-binding protein 1c and fatty acid synthetase. Moreover, other cytokines induced by alcohol (e.g. IL-6) might also impair the transport and secretion of TG. Thus, GZP intervention might reduce steatosis by reducing levels of the pro-inflammatory cytokines TNF-α and IL-6 in liver cells (Fig. 5). These results showed that GZP significantly improved alcohol-induced blood lipid disorders in rats, and no significant difference was found between all GZP groups and the normal control group ($P > 0.05$), suggesting that GZP represents a potential therapeutic agent for commercial or pharmaceutical applications.

3.5.3. GZP improves alcohol-induced oxidative stress in liver cells

Oxidative stress generated by alcohol metabolism is reportedly a major driver of alcohol-induced liver damage (Sugimoto & Takei, 2017). To assess the redox status of rat livers and the liver-protective antioxidant effects of GZP, the ROS level, the activities of endogenous antioxidant enzymes, and GSH content in rat livers were measured (Table 3).

Table 3 shows that the model group displayed significantly lower SOD, GSH-Px, GSR activities and GSH content, as well as significantly elevated ROS content ($P < 0.01$), compared with the normal group. Specifically, ROS level was increased by 47.40%, whereas SOD, GSH-Px, GSR activities, and GSH content were decreased by 56.43%, 24.95%, 57.51%, and 49.39%, respectively. These parameters indicate that alcohol exposure led to the excessive production of ROS and the depletion of endogenous antioxidant enzymes and GSH content (i.e. alcohol-induced oxidative stress in the liver cells).

In this study, it was found that alcohol-induced changes in redox status were significantly mitigated by GZP administration. The results showed that medium and high doses of GZP restored normal ROS levels, whereas low doses did not achieve the same effect. In particular, ROS level in the high-dose GZP group was lower than that attained by administration of the same concentration of ZP, this result possibly related to the improved free radical-scavenging ability of ZP following glycosylation.

GSH constitutes the first line of defense against free radicals in living organisms and is a substrate for GSH-Px and GSR; therefore, GSH content is an important measure of antioxidant capacity. Compared to that in the model group, GSH content in livers of all GZP groups was markedly increased ($P < 0.05$–0.01). Specifically, GSH content was increased by 80.75% following GZP administration at 500 mg/kg·bw, which was higher than that in the ZP group at the same dose. The significant increase in GSH content might be attributed to GZP-induced increases in GSH-Px and GSR activities at a dose of 500 mg/kg·bw GZP (by 27.32% and 80.96%, respectively, compared to those in the model group and 23.46% and 45.26%, respectively, compared to those with the same dose of ZP). These results indicate that GZP accelerated the conversion of GSSG to GSH and increased the GSH:GSSG ratio, down-regulated levels of hydrogen peroxide, and thereby alleviated alcohol-induced hepatic oxidative stress.

SOD is a superoxide anion radical scavenging factor and among the most important internal antioxidases. GZP administration at all doses significantly ameliorated reductions in alcohol-induced SOD activity. Compared with the model group, SOD activity in the high-dose GZP group increased significantly ($P < 0.05$) by 68.26%, which was 11.19% higher than that in the 500 mg/kg·bw ZP group, suggesting that GZP was more effective than ZP at alleviating superoxide anion radical-induced oxidative stress in liver cells.

The experimental results showed that GZP intervention could reverse oxidative damage in liver cells by improving the activities of antioxidant enzymes, such as SOD, GSH-Px, and GSR, as well as by increasing GSH content. These antioxidant enzymes can be induced by nuclear factor erythroid 2-related factor-2 (Nrf2), which can upregulate the transcription of antioxidant enzymes (such as SOD, GSH-Px, and GSR) and improve the ability of anti-oxidative stress. Herein we found that GZP significantly increased SOD, GSH-Px, and GSR activities, as compared to those in the model group, which might indicate that GZP activates Nrf2 in rat livers. Further studies are being conducted to investigate whether Nrf2 is a direct target of GZP. Lv et al. (2013) reported that the hepatoprotective effect of CP derived from concentrated corn proteins on thioacetamide-induced hepatic fibrosis could be attributed to its antioxidant capabilities. Additionally, Zhang, Zhang, and Li (2012) reported similar findings concerning the protective effects of corn oligopeptides from CGM on early alcoholic liver injury. Moreover, several recent studies showed that CP possesses excellent *in vitro* antioxidant activities (e.g. free-radical scavenging ability, metal-ion chelating capacity, and reducing power) (Jiang et al., 2018; Ren, Liang, et al., 2018; Wang et al., 2018). Similarly, it was observed in this study that the covalent conjugation of D-glucosamine to ZP enhanced its antioxidant capacity. Therefore, the antagonistic effects of GZP against alcohol-induced liver injury can be attributed, at least partially, to its free radical-scavenging ability and reducing power (data not shown), which enhanced hepatocyte antioxidant capacity and alleviated a series of metabolic changes linked to oxidative stress, including mitochondrial dysfunction, steatosis, inflammation and fibrosis.

3.5.4. GZP ameliorates alcohol-induced abnormal cytokine expression

Excessive alcohol consumption leads to the overexpression of

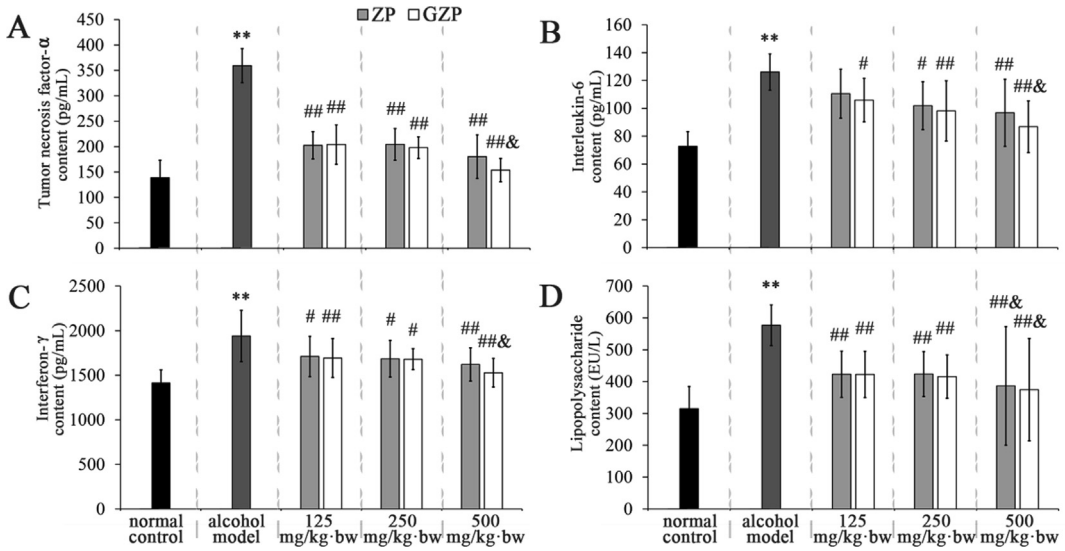

Fig. 5. Effects of GZP on serum contents of TNF-α (A), IFN-γ (B), IL-6 (C) and liver content of LPS (D) in alcohol-induced Wister rats fed a diet containing GZP for 28 days. Data are expressed as the mean ± SD, and differences were analyzed by Tukey's test, n = 10. * $P < 0.05$ and ** $P < 0.01$ vs the normal control group, # $P < 0.05$ and ## $P < 0.01$ vs the alcohol model group, & $P > 0.05$ vs the normal control group, ^ $P < 0.05$ vs the same concentration of ZP.

various cytokines that act as inflammatory mediators, which can induce hepatocyte dysfunction, apoptosis, necrosis, and fibrosis (McClain, Song, Barve, Hill, & Deaciuc, 2004). The effect of GZP on the content of serum cytokines in rats is shown in Fig. 5. The contents of the hepatic pro-inflammatory cytokines TNF-α, IL-6, and IFN-γ in the alcohol-treated group were significantly elevated compared to those in the normal control group ($P < 0.01$), suggesting that chronic alcohol exposure led to abnormal cytokine metabolism in hepatocytes. These molecules can cause inflammatory liver injury with increased endoplasmic reticulum stress and mitochondrial dysfunction. It was subsequently observed the dose-dependent attenuation of these levels following GZP or ZP treatment. In particular, following GZP or ZP treatment at 500 mg/kg·bw, cytokine levels returned to normal. Furthermore, reductions in cytokine levels in the GZP group were more pronounced than those in the ZP group.

Previous studies demonstrated that cytokine production induced by long-term alcohol exposure is triggered by gut-derived LPS and reactive oxygen intermediates (ROIs), and that LPS and ROIs induce cytokine production by activating the redox-sensitive nuclear factor-kappa B (NF-κB) signaling pathway in Kupffer cells; meanwhile, pro-inflammatory cytokines can promote ROS generation (McClain et al., 2004, Manoranjan, 2018). Fig. 5d shows the effect of GZP treatment on LPS content in the rat liver. The results indicated significantly higher LPS content in the model group relative to that in the normal group ($P < 0.01$), suggesting that alcohol intake enhanced intestinal permeability and led to the leakage of LPS. However, groups treated with GZP, especially high-dose GZP, exhibited significantly lower LPS levels than the model group, with high-dose GZP and ZP treatment reducing LPS content by 35.08% and 33.03%, respectively, relative to that in the model group. Further, no significant differences were observed between these two groups and the normal control group ($P > 0.05$).

It was shown that respective GZP and ZP administration enhanced the total antioxidant capacity of liver cells; therefore, GZP and ZP supplementation might decrease activation of NF-κB signaling induced by LPS and ROIs, in addition to downregulating the production of pro-inflammatory cytokines, thereby blocking the development of inflammation and alleviating a series of metabolic changes linked to inflammation, including oxidative stress, steatosis, and lipid peroxidation. Our results agree with those reported by Ren, Geng, et al. (2018), who found that *Coriolus versicolor*-derived polysaccharide peptides can attenuate NF-κB signaling by reducing LPS content, thereby significantly reducing alcohol-induced inflammatory responses. Therefore, our results suggest that the liver-protective effects of GZP are related to attenuated inflammatory responses, although additional studies are required to elucidate the mechanisms by which GZP inhibits NF-κB signaling pathway.

Table 3
Effect of GZP on activities of endogenous antioxidant enzymes and GSH content.

Treatment groups	ROS (U/mL)	SOD (U/mL)	GSR (mIU/mL)	GSH-Px (U/L)	GSH (mmol/L)
Normal control	243.82 ± 41.09	199.00 ± 35.49	178.80 ± 38.04	117.89 ± 11.22	295.76 ± 26.34
Alcohol model	359.40 ± 33.62**	86.70 ± 19.28**	75.98 ± 25.49**	88.48 ± 12.21**	149.67 ± 45.96**
ZP(125 mg/kg·bw)	319.31 ± 67.61	104.37 ± 9.18	99.03 ± 21.29	103.39 ± 15.43	211.50 ± 19.34##
ZP(250 mg/kg·bw)	316.24 ± 57.21	128.46 ± 26.82#	108.80 ± 31.35	109.31 ± 17.69# &	221.24 ± 51.69##
ZP(500 mg/kg·bw)	288.7 ± 50.35# &	136.18 ± 37.29##	110.37 ± 38.89	109.24 ± 12.82# &	242.65 ± 31.07##
GZP(125 mg/kg·bw)	328.30 ± 45.75	139.68 ± 21.40## &	109.71 ± 30.58	105.69 ± 18.43	228.01 ± 49.29##
GZP(250 mg/kg·bw)	277.54 ± 52.00## &	136.62 ± 9.09##	119.13 ± 22.37#	109.54 ± 16.85# &	239.55 ± 42.88##
GZP(500 mg/kg·bw)	261.87 ± 12.18## &	145.88 ± 22.69##	137.49 ± 23.85##	112.66 ± 16.75# &	270.53 ± 30.96## &

Data are expressed as the mean ± SD, n = 10.
*$P < 0.05$ and,
** $P < 0.01$ vs the normal control group,
# $P < 0.05$ and,
$P < 0.01$ vs the model group,
& $P > 0.05$ vs the normal control group.

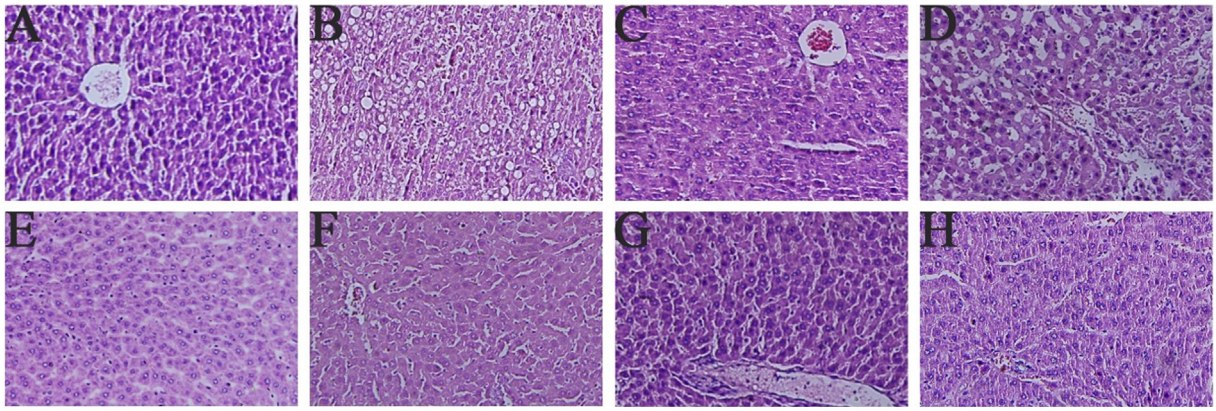

Fig. 6. Histopathological sections of the livers (H&E, ×400). (A) normal control group; (B) alcohol model group; (C) 125 mg/kg·bw of GZP + alcohol; (D) 125 mg/kg·bw of ZP + alcohol; (E) 250 mg/kg·bw of GZP + alcohol; (F) 250 mg/kg·bw of ZP + alcohol; (G) 500 mg/kg·bw of GZP + alcohol; (H) 500 mg/kg·bw of ZP + alcohol.

3.5.5. GZP mitigates alcohol-induced pathological changes in liver tissue

The hepatoprotective effect of GZP was further confirmed via histopathological examination (Fig. 6). Liver cells from the normal control group were characterized by intact structures, dense arrangements, balanced staining, and the absence of pathological changes such as lipid droplet accumulation (Fig. 6A). In contrast, steatosis was observed in some liver cells from rats subjected to continuous alcohol administration, which was characterized by the accumulation of lipid droplets of various sizes in the cytoplasm and translocation of the nucleus to the cell periphery, which is consistent with characteristics of early alcoholic liver disease (Fig. 6B). These pathological changes suggested that alcohol stimulation caused severe liver damage. However, compared with the model group, intervention with GZP and ZP supplementation significantly alleviated alcohol-induced pathological changes in the liver (Fig. 6C-H). Low-dose ZP intervention alleviated steatosis, although certain pathological changes such as irregular hepatic cord arrangement and swollen hepatocytes were still visible (Fig. 6D). Additionally, medium doses of ZP significantly reduced hepatocyte swelling and promoted the maintenance of relatively regular morphology, whereas high doses of ZP restored hepatocyte morphology similar to that observed in the normal group. Following GZP intervention, dose-dependent reductions in liver-cell injury were observed, as the low-dose GZP group displayed a few small lipid droplets in the cytoplasm, whereas medium- to high-dose GZP reversed alcohol-induced hepatic lobule injuries and enabled the restoration of liver tissue to that observed in the normal group. These histological observations were consistent with the results obtained by measuring biochemical indices and support our findings that GZP exhibits significant liver-protective effects.

4. Conclusions

In this study, GZP was prepared through the TGase-mediated conjugation of D-glucosamine. Compared to ZP, GZP displayed superior capacity for promoting alcohol metabolism activities both *in vitro* and *in vivo*. Moreover, in a rat model of alcohol-induced liver injury, significant GZP-mediated dose-dependent improvements in biochemical indices and liver histopathology associated with alcohol-induced liver injury were demonstrated. Specifically, GZP administration at 250 mg/kg·bw alleviated alcohol-induced liver injury parameters in the rat model restoring levels to those observed in normal control. Our results support the fact that GZP has excellent potential for functional food or dietary supplementation to protect against alcohol-induced liver injury.

Ethics Statement

Animal handling was performed in accordance with the *Guide for the Care and Use of Laboratory Animals* published by the U.S. National Institutes of Health (NIH Publication No. 85-23, 1996 revision).

CRediT authorship contribution statement

Xiao-jie Wang: Investigation and Writing - review & editing. **Xiao-lan Liu:** Data curation and Writing - review & editing. **Xi-qun Zheng:** Funding acquisition. **Yue Qu:** Investigation. **Yan-guo Shi:** Project administration.

Declaration of Competing Interest

The authors declare that they have no known competing financial interests or personal relationships that could have appeared to influence the work reported in this paper.

Acknowledgments

This work was supported by the National Key Research and Development Program of China (2017YFD0400200), the Foundation for the Characteristic Discipline of Processing Technology of Plant Foods (YSTSXK201819), and the Fundamental Research Funds of Department of Education of Heilongjiang Province (135309345), and the Heilongjiang Touyan Innovation Team Program.

References

Chen, L., Ullah, N., Li, C. Y., Hackman, R. M., Li, Z. X., Xu, X. L., ... Feng, X. C. (2017). Incorporated glucosamine adversely affects the emulsifying properties of whey protein isolate polymerized by transglutaminase. *Journal of Dairy Science, 100*(5), 3413–3423. https://doi.org/10.3168/jds.2016-12071.

Chen, X., & Wang, S. Y. (2019). Cryoprotective effect of antifreeze glycopeptide analogues obtained by nonenzymatic glycation on *Streptococcus thermophilus* and its possible action mechanism. *Food Chemistry, 288*, 239–247. https://doi.org/10.1016/j.foodchem.2019.03.011.

Gioia, L. D., Cuq, B., & Guilbert, S. (1998). Effect of hydrophilic plasticizers on thermomechanical properties of corn gluten meal. *Cereal Chemistry, 75*(4), 514–519. https://doi.org/10.1094/CCHEM.1998.75.4.514.

Guo, H., Sun, J., He, H., Yu, G. C., & Du, J. (2009). Antihepatotoxic effect of corn peptides against Bacillus Calmette-Guerin/lipopolysaccharide-induced liver injury in mice. *Food and Chemical Toxicology, 47*, 2431–2435. https://doi.org/10.1016/j.fct.2009.06.041.

Haseba, T., Duester, G., Shimizu, A., Yamamoto, I., Kameyama, K., & Ohno, Y. (2006). *In vivo* contribution of class III alcohol dehydrogenase (ADH 3) to alcohol metabolism through activation by cytoplasmic solution hydrophobicity. *Biochimica et Biophysica Acta-biomembranes, 1762*, 276–283. https://doi.org/10.1016/j.bbadis.2005.11.008.

Hong, P. K., Gottardi, D., Ndagijimana, M., & Betti, M. (2016). Glucosamine-induced glycation of hydrolysed meat proteins in the presence or absence of transglutaminase: Chemical modifications and taste-enhancing activity. *Food Chemistry, 197*, 1143–1152. https://doi.org/10.1016/j.foodchem.2015.11.096.

Hrynets, Y., Ndagijimana, M., & Betti, M. (2014). Transglutaminase-catalyzed glycosylation of natural actomyosin (NAM) using glucosamine as amine donor: Functionality

and gel microstructure. *Food Hydrocolloids, 36*(5), 26–36. https://doi.org/10.1016/j.foodhyd.2013.09.001.

Jiang, S. J., & Zhao, X. H. (2010). Transglutaminase-induced cross-linking and glucosamine conjugation in soybean protein isolates and its impacts on some functional properties of the products. *European Food Research and Technology, 231*(5), 679–689. https://doi.org/10.1007/s00217-010-1319-2.

Jiang, Y., Zhang, M. D., Lin, S. Y., & Cheng, S. (2018). Contribution of specific amino acid and secondary structure to the antioxidant property of corn gluten proteins. *Food Research International, 105*, 836–844. https://doi.org/10.1016/j.foodres.2017. 12.022.

Kawada, T., Masaki, H., Mori, M., & Torii, K. (1988). Change of preference for L-amino acids in rats ingested ethyl alcohol chronically. *Proceedings of the 22nd Japanese Symposium on Taste and Smell* (pp. 225–228). .

Kieliszek, M., & Misiewicz, A. (2014). Microbial transglutaminase and its application in the food industry: A review. *Folia Microbiologica, 59*(3), 241–250. https://doi.org/10.1007/s12223-013-0287-x.

Kumar, D., Dwivedi, D. K., Lahkar, M., & Jangra, A. (2019). Hepatoprotective potential of 7,8-dihydroxyflavone against alcohol and high-fat diet induced liver toxicity via attenuation of oxido-nitrosative stress and NF-κB activation. *Pharmacological Reports, available online*. https://doi.org/10.1016/j.pharep.2019.07.002.

Lv, J., Nie, Z. K., Zhang, J. L., Liu, F. Y., Wang, Z. Z., Ma, Z. L., & He, H. (2013). Corn peptides protect against thioacetamide-induced hepatic fibrosis in rats. *Journal of Medicinal Food, 16*(10), 912–919. https://doi.org/10.1089/jmf. 2012.2626.

Manoranjan, A. (2018). Protective role of antioxidants in alcoholic liver disease. *Med Phoenix, 3*(1), 75–88. https://doi.org/10.3126/medphoenix.v3i1.20767.

Ma, Z. L., Hou, T., Shi, W., Liu, W. W., & He, H. (2015). Inhibition of hepatocyte apoptosis: An important mechanism of corn peptides attenuating liver injury induced by ethanol. *International journal of molecular sciences, 16*(9), 22062–22080. https://doi.org/10.3390/ijms160922062.

McClain, C. J., Song, Z. Y., Barve, S. S., Hill, D. B., & Deaciuc, I. (2004). Recent advances in alcoholic liver disease IV. dysregulated cytokine metabolism in alcoholic liver disease. *The American Journal of Physiology-Gastrointestinal and Liver Physiology, 287*, 497–502. https://doi.org/10.1152/ajpgi.00171.2004.

Paluszkiewicz, C., Stodolak, E., Hasik, M., & Blazewicz, M. (2011). FT-IR study of montmorillonite-chitosan nanocomposite materials. *Spectrochimica Acta Part A: Molecular and Biomolecular Spectroscopy, 79*(4), 784–788. https://doi.org/10.1016/j.saa.2010.08.053.

Pomes, A. F. (1971). Zein. *The encyclopedia of polymer science and technology: Vol. 5*, (pp. 125–132). New York: John Wiley and Sons.

Ren, X. F., Liang, Q. F., Zhang, X., Hou, T., Li, S. Y., & Ma, H. L. (2018). Stability and antioxidant activities of corn protein hydrolysates under simulated gastrointestinal digestion. *Cereal Chemistry, 95*(6), 760–769. https://doi.org/10.1002/cche.10092.

Ren, Y. L., Geng, Y., Chen, H. D., Lu, Z. M., Shi, J. S., & Xu, Z. H. (2018). Polysaccharide peptides from *Coriolus versicolor*: A multi-targeted approach for the protection or prevention of alcoholic liver disease. *Journal of Functional Foods, 40*, 769–777. https://doi.org/10.1016/j.jff.2017.11.051.

Shi, J., & Zhao, X. H. (2019). Effect of caseinate glycation with oligochitosan and transglutaminase on the intestinal barrier function of the tryptic caseinate digest in IEC-6 cells. *Food & Function, 10*(2), 652–664. https://doi.org/10.1039/C8FO01785A.

Song, C. L., & Zhao, X. H. (2013). Rheological, gelling and emulsifying properties of a glycosylated and cross-linked caseinate generated by transglutaminase. *International Journal of Food Science and Technology, 48*(12), 2595–2602. https://doi.org/10.1111/ijfs.12255.

Sugimoto, K., & Takei, Y. (2017). Pathogenesis of alcoholic liver disease. *Hepatology Research, 47*(1), 70–79. https://doi.org/10.1111/hepr.12736.

Vallee, B. L., & Hoch, F. L. (1955). Zinc: A component of yeast alcohol dehydrogenase. *Proceedings of the National Academy of Sciences of the United States of America, 41*(6), 327–328. https://doi.org/10.1073/pnas.41.6.327.

Wang, L., Ding, L., Xue, C., Ma, S., Du, Z., Zhang, T., & Liu, J. (2018). Corn gluten hydrolysate regulates the expressions of antioxidant defense and ROS metabolism relevant genes in H_2O_2-induced HepG2 cells. *Journal of Functional Foods, 42*, 362–370. https://doi.org/10.1016/j.jff.2017.12.056.

Wang, Xiao-jie, Zheng, Xi-qun, Kopparapu, Narasimha-kumar, Cong, Wan-suo, Deng, Yong-ping, Sun, Xiu-jiao, & Liu, Xiao-lan (2014). Purification and evaluation of a novel antioxidant peptide from corn protein hydrolysate. *Process Biochemistry, 49*(9), 1562–1569. https://doi.org/10.1016/j.procbio.2014.05.014.

Wang, X. J., Zheng, X. Q., Liu, X. L., Kopparapu, N. K., Cong, W. S., & Deng, Y. P. (2017). Preparation of glycosylated zein and retarding effect on lipid oxidation of ground pork. *Food Chemistry, 227*, 335–341. https://doi.org/10.1016/j. foodchem. 2017.01.069.

Yamaguchi, M., Takada, M., Nozaki, O., Ito, M., & Furukawa, Y. (1996). Preparation of corn peptide from corn gluten meal and its administration effect on alcohol metabolism in stroke-prone spontaneously hypertensive rats. *Journal of Nutritional Science and Vitaminology, 42*, 219–231. https://doi.org/10.3177/jnsv.42.219.

Yamaguchi, M., Nishikiori, F., Ito, M., & Furukawa, Y. (1997). The effects of corn peptide ingestion on facilitating alcohol metabolism in healthy men. *Bioscience, Biotechnology and Biochemistry, 61*(9), 1474–1481. https://doi.org/10.1271/bbb. 61.1474.

Yang, S. C., Ito, M., Morimatsu, F., Furukawa, Y., & Kimura, S. (1993). Effects of amino acids on alcohol intake in stroke-prone spontaneously hypertensive rats. *Journal of Nutritional Science and Vitaminology, 39*, 55–61. https://doi.org/10.3177/jnsv.39.55.

Yao, X. T., & Zhao, X. H. (2016). Pre-deamidation of soy protein isolate exerts impacts on transglutaminase-induced glucosamine glycation and cross-linking as well as properties of the products. *Journal of the Science of Food and Agriculture, 96*(7), 2418–2425. https://doi.org/10.1002/jsfa.7361.

Yu, G. C., Li, J. T., He, H., Huang, W. H., & Zhang, W. J. (2013). Ultrafiltration preparation of potent bioactive corn peptide as alcohol metabolism stimulator *in vivo* and study on its mechanism of action. *Journal of Food Biochemistry, 37*, 161–167. https://doi.org/10.1111/j.1745-4514.2011.00613.x.

Yuan, F. Z., Lv, L. T., Li, Z. X., Mi, N. S., Chen, H. R., & Lin, H. (2017). Effect of transglutaminase-catalyzed glycosylation on the allergenicity and conformational structure of shrimp (*Metapenaeus ensis*) tropomyosin. *Food Chemistry, 219*, 215–222. https://doi.org/10.1016/j.foodchem.2016.09.139.

Zhang, F., Zhang, J. L., & Li, Y. (2012). Corn oligopeptides protect against early alcoholic liver injury in rats. *Food and Chemical Toxicology, 50*(6), 2149–2154. https://doi.org/10.1016/j.fct.2012.03.083.

Zhou, C. S., Ma, H. L., Ding, Q. Z., Lin, L., Yu, X. J., Luo, L., ... Yagoub, A. E. G. A. (2013). Ultrasonic pretreatment of corn gluten meal proteins and neutrase: Effect on protein conformation and preparation of ACE (angiotensin converting enzyme) inhibitory peptides. *Food and Bioproducts Processing, 91*(4), 665–671. https://doi.org/10.1016/j.fbp.2013.06.003.

Zhou, L. M., Liu, X. L., Liu, Y., & Zheng, X. Q. (2014). TGase-catalyzed glycosylation of zein. *Food Science, 35*(24), 15–19. https://doi.org/10.7506/spkx1002-6630-201424003.

Zhu, B. Y., He, H., & Hou, T. (2019). A comprehensive review of corn protein-derived bioactive peptides: Production, characterization, bioactivities, and transport pathways. *Comprehensive Reviews in Food Science and Food Safety, 18*(1), 329–345. https://doi.org/10.1111/1541-4337.12411.